

Pheromone-Diffusion-based Conscientious Reactive Path Planning for Road Network Persistent Surveillance *

Tong Wang, Gangqi Dong, and Panfeng Huang, *Senior Member, IEEE*

Abstract— **Road Network Persistent Surveillance Problem (RPSP)** involves path planning for an unmanned ground vehicle (UGV) with detection ability to timely detect the events randomly occurred. The road network is formed by edges and weighted viewpoints, where the UGV must move along the edges. The existing method based on cognitive architecture is inadequate in terms of real-time and effective decision making. To improve the computation efficiency and accuracy of solving RPSP, a new algorithm called Pheromone-Diffusion-based Conscientious Reactive Persistent Surveillance (PD-CRPS) is proposed in this paper. Considering the detection ability of UGV, the monitoring weight, the surveillance effect, and the topology of the road network, a model of pheromone release and diffusion is established to estimate the global uncertainty through the local information around the UGV. The local optimum avoidance technology based on pheromone is designed, and the reactive architecture is used to design the payoff function of decision making. The worst-case computational time complexity of the PD-CRPS is far less than the existing cognitive architecture method. Simulation results show that the PD-CRPS can not only efficiently plan the path of UGV in the road networks with different topologies and observation obstacles, but also improve the calculation accuracy.

I. INTRODUCTION

Unmanned ground vehicle (UGV) is important application tool in the field of security monitoring [1, 2]. In the environment where UGV generally works, the road width of most reachable areas is smaller than the diameter of the detection range of UGV. Such an environment can be abstracted as an undirected graph, which is a network composed of viewpoints and segment paths (or edges) [3]. Path planning for UGV on road network with certain detection ability is an important subject of security monitoring.

Wang *et al.* [4] presented a security monitoring problem of UGV with detection ability on the road network - the Road Network Persistent Surveillance Problem (RPSP). This problem comes from the non-adversarial surveillance or patrolling tasks by mobile robot in area with “significant” road network in reality [4]. Unlike non-persistent problems such as exploration [5] and coverage [6], in RPSP, UGV must continuously and repeatedly monitor the road network. Compared with the general surveillance problem, RPSP has two features: a) the UGV must move along the edge and make a decision about the next direction when it reaches a viewpoint;

*Resrach supported in part by the National Natural Science Foundation of China (Grant Nos. 61725303 and 61803312). (Corresponding author: Gangqi Dong)

The authors are with the Research Center for Intelligent Robotics, the School of Astronautics, Northwestern Polytechnical University, Xi'an, Shaanxi, China, and with the National Key Laboratory of Aerospace Flight Dynamics, Northwestern Polytechnical University, Xi'an, Shaanxi, China (e-mail: tongwang@mail.nwpu.edu.cn, pfhuang@nwpu.edu.cn, and dong@nwpu.edu.cn).

b) the UGV moving on the road network has a limited coverage - UGV can simultaneously monitor multiple viewpoints in the neighborhood on a viewpoint. The former feature distinguishes RPSP from existing problems such as 1-D persistent surveillance [7], 2-D persistent surveillance [8], and dynamic coverage [9]. The latter feature distinguishes RPSP from the problems based on the undirected graph such as multi-robot patrolling [10] and the optimal watchman route problem based on lines [11]. For the specific differences between RPSP and other problems as well as the existing solutions to other problems, please refer to the Ref. [4, 12-14].

Inspired by the general conclusion in the patrolling problem [15], a heuristic path planning method based on cognitive architecture called Road-network Persistent Surveillance (RPS) [4] is designed to solve RPSP. Although it can implement weighted persistent surveillance of UGV in road networks of any topology, it still has two imperfections:

a) The cognitive architecture must consider the cost of UGV to each viewpoint [16], so it is necessary to calculate the shortest path to each viewpoint, which makes the worst-case complexity as high as $O(N^3)$, where N is the number of all viewpoints. As the number of viewpoints increases, the calculation time of RPS will increase significantly.

b) A special heuristic rule is designed to avoid local optimum by suppressing the backtracking of UGV between two viewpoints with a certain probability. However, this rule cannot distinguish whether the UGV is in normal backtracking or trapped in a local optimum. When the normal backtracking occurs, the suppression will hurt harm the surveillance effect.

The motivation of this paper is to propose a dynamic planning method with low computational time complexity and high accuracy to plan the path along the road network for UGV with certain detection ability to improve the efficiency and accuracy of solving RPSP.

Previous studies have shown that the reactive methods based on the greedy strategy have low computational time complexity, which is very suitable for real-time planning [17-21]. However, the reactive methods often fail to obtain the result equivalent to the effect of the cognitive methods because of the lack of global information [16]. Therefore, how to estimate the global state based on local information is the key to the reactive method to tackle RPSP.

Think of an optimization algorithm based on the greedy strategy - Ant Colony Algorithm (ACO) [22]. Inspired by the process of ant colony exploring food, the diffusion enables a “shortsighted” ant to perceive the information in larger spaces or farther away [23], so as to estimate its position in local or even global. Numerous examples have also demonstrated the optimization ability of ACO in complex constraint problems [24, 25]. Therefore, according to the diffusion of pheromone, the method for estimating the global surveillance effect based on local information can be designed.

Main Contributions: a) A pheromone diffusion model suitable for RPSP is designed to reflect the global monitoring uncertainty information on a single viewpoint to estimate the global surveillance effect based on local information; b) A simple pheromone-based local optimum avoidance technique is proposed. It changes the distribution of the pheromone by modifying the model parameters in the pheromone calculation to guide the UGV to avoid the local optimum, without using special rules that explicitly suppress backtracking; c) A new algorithm called Pheromone-Diffusion-based Conscientious Reactive Persistent Surveillance (PD-CRPS) is proposed, of which time complexity is at least two orders of magnitude less than the existing method. The simulation show that the PD-CRPS can not only efficiently plan the path of UGV on road networks with different topologies and observation obstacles, but also improve the calculation accuracy.

II. PRELIMINARIES AND PROBLEM STATEMENT

A. Environment and UGV Model

The environment of UGV monitoring is modeled as an time-invariant undirected graph composed of viewpoints and edges $G = (V, E, D, W)$, where $V = \{v_1, v_2, \dots, v_N\}$ is the viewpoint set, (x_i, y_i) is the coordinate of $v_i \in V$, N is the number of the viewpoints, $E = \{e_1, e_2, \dots, e_M\}$ is the edge set, M is the number of the edges, $E_{i,j} \in E$ represents the connection relationship between v_i and v_j , $E_{i,j} = 1$ means that they are adjacent points, i.e. there is no need to pass through other viewpoints from v_i to v_j , $D = \{d_1, d_2, \dots, d_M\}$ is distance set, $\|D_{i,j}\|$ represents the length of the edge between v_i and v_j , $W = \{\sigma_1, \sigma_2, \dots, \sigma_N\}$ is the monitoring weight matrix which represents the importance of each viewpoint, $\forall \sigma_i \in W, \sigma_i \geq 1$.

The UGV has the ability of moving and detecting. Its movement ability is described by a discrete dynamic equation

$$P(t + t_d) = \begin{cases} P_x(t) + v_u t_d \cos \theta(t) \\ P_y(t) + v_u t_d \sin \theta(t) \end{cases}, \quad (1)$$

where $P(t) = (P_x(t), P_y(t))$ represents the location of UGV at time t , v_u is the constant speed of UGV and the speed change when UGV turning is not considered, t_d is a discrete time step, $\theta(t)$ represents the angle between the UGV's moving direction $\theta(t)$ and the x coordinate axis at time t .

The detection ability of UGV reflects the detection accuracy of the UGV to the event occurred at the position with different distance from the UGV in the detection range, which is expressed by a piecewise probability function

$$f_c = \begin{cases} 1, & d_s \leq d_c \\ (d_c - d_s) / (d_L - d_c) + 1, & d_c < d_s \leq d_L \\ 0, & d_s > d_L \end{cases}, \quad (2)$$

where d_s is the distance from a certain position in the environment to UGV, d_c represents the observation radius of UGV, d_L is the detection limitation of UGV. It should be noted that $f_c = 0$ if there is an observation obstacle between the sensor center and a certain position whose $d_s \leq d_L$. It is assumed that the observation obstacle is static and time-invariant.

B. RPSP

In RPSP, the UGV with detection ability continuously moves along the edges of the road network to monitor each

viewpoint and detect whether there are random events occurring at the viewpoint. The time and location of each occurrence are unknown while the duration of each occurrence is a priori [26]. The monitoring uncertainty [27] is used to represent the non-confidence level of event status at the viewpoint. The monitoring uncertainty [4] of the i -th viewpoint at time t is expressed as

$$u_i(t) = \begin{cases} 0, & f_c = 1 \\ \sigma_i(t - t_{di})(1 - f_c) / t_{lim}, & \text{otherwise,} \\ 1, & u_i(t) > 1 \end{cases} \quad (3)$$

where t_{di} represents the time when the i -th viewpoint was last fully monitored, $-u_i(t) = 0, t - t_{di} = 0$, t_{lim} is the expected time, reflecting the minimum prior duration of all random events on the road network. Readers are invited to refer to [4] for more detailed explanation of monitoring uncertainty.

The surveillance effect is evaluated through the following three criteria, including the average uncertainty

$$C_1 = \frac{1}{N} \sum_{i=1}^N u_i(t), \quad (4)$$

the stable mean of global uncertainty

$$C_2 = \frac{1}{T - t_w + 1} \sum_{t=t_w}^T \sum_{i=1}^N u_i(t), \quad (5)$$

and the stable variance of uncertainty

$$C_3 = \sqrt{\frac{1}{T - t_w + 1} \sum_{t=t_w}^T \left(\sum_{i=1}^N u_i(t) - C_2 \right)^2}, \quad (6)$$

where t_w is stable time, which means the beginning time when UGV exactly executes a whole traversal coverage, T is the mission duration.

The RPSP is formulated as a function f , i.e.

$$f = \arg \min_{X_T} (C_2), \quad (7)$$

by finding a path for continuous movement of the UGV represented by a viewpoint set $X_T = \{v_a, v_b, \dots\}, v_a, v_b, \dots \in V$, subject to v_u, f_c , and $G = (V, E, D, W)$.

III. ESTIMATION OF GLOBAL UNCERTAINTY BASED ON PHEROMONE

To design the estimation model of global monitoring uncertainty state through limited local information based on pheromone, the following three questions need to be answered: what is the pheromone that needs to be diffused, how does the pheromone diffuse in road network, and how pheromones act on viewpoints after diffusing. The following three subsections elaborate and answer these three questions respectively.

A. Releasing Pheromone

There are two kinds of pheromone at a viewpoint, which are the pheromone produced by itself (Releasing Pheromone) and the pheromone diffused by others (Diffused Pheromone). Diffused pheromone is essentially formed by the joint action of releasing pheromone from multiple viewpoints. Therefore, releasing pheromone is the basis of the estimation model of

global monitoring uncertainty based on the pheromone. The weighted average monitoring uncertainty of all the observable viewpoints [4] is used as the releasing pheromone of a single viewpoint. Fig. 1 illustrates the definition of the observable viewpoints of a viewpoint. In particular, to enable UGV to move to the viewpoint with the maximum monitoring uncertainty, the releasing pheromone of this viewpoint is set to its monitoring uncertainty, as the major diffusion source of the pheromone. Therefore, the releasing pheromone of v_i is

$$p_i^r = \begin{cases} \frac{1}{\|O_{vi}\|} \sum_{j \in O_{vi}} u_j(t)/\sigma_j, & u_i(t) \neq u_{\max}, \\ u_{\max}, & u_i(t) = u_{\max} \end{cases}, \quad (8)$$

where p_i^r is the releasing pheromone of the v_i , O_{vi} is the observable viewpoints set of the v_i , $\|O_{vi}\|$ is the number of viewpoints in O_{vi} , $u_j(t)$ is the monitoring uncertainty of v_j in O_{vi} at time t , and u_{\max} is the maximum monitoring uncertainty of all viewpoint at time t . Using the reciprocal weighting of the monitoring weights can reflect the time interval between two full monitoring around the viewpoints.

B. Diffused Pheromone

We adopt a multi-source diffusion method so that each viewpoint diffuses pheromone outward along the edge. Inspired by the swarm intelligent patrol method [23], we set the diffused pheromone of a viewpoint as: the maximum value of the diffused pheromone of all adjacent viewpoints received by this viewpoint, i.e.

$$p_i^d = \arg \max \left(\left\{ PU(i, j) : \|D_{i,j}\| \neq \infty \cap i \neq j \right\} \right), \quad (9)$$

where $\|D_{i,j}\| \neq \infty$ indicates that the v_j is the adjacent viewpoint of the v_i , and $PU(i, j)$ is the pheromone diffused from viewpoint j and received by v_i , it is

$$PU(i, j) = \begin{cases} p_j^s - C_d(i, j) - \beta I_i(t), & PU(i, j) \geq p_m \\ p_m, & PU(i, j) < p_m \end{cases}, \quad (10)$$

where p_j^s is the synthetic pheromone of the v_j , $C_d(i, j)$ is the diffusion loss, β is the absorption coefficient, $I_i(t)$ is the absorption factor of the i -th viewpoint at time t , and $p_m \geq 0$ is the minimum diffusion value. The definition and meaning of the above variables are elaborated in the followings.

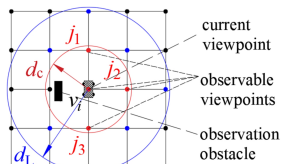


Fig. 1 The observable viewpoints. In cases free of observation obstacle, the viewpoint can be fully monitored when the distance between the UGV and it is no more than d_c . Otherwise, the viewpoint can not be fully monitored.

Firstly, the diffusion loss $C_d(i, j)$ is described, which represents the numerical loss of the synthetic pheromone when it diffuses between the v_i and v_j . It takes time for pheromone to diffuse between viewpoints, which is equivalent to the time consumption of the UGV moving from v_j to v_i . We assume that the higher the monitoring weight, the smaller the loss of diffusion. This time consumption is formulated as

$$C_d(i, j) = \frac{c_L \|D_{i,j}\|}{v_u t_{\lim} \sigma_i}, \quad (11)$$

where c_L is the loss coefficient, which is artificially set up to control the diffusion speed of the pheromone.

The purpose of setting the absorption coefficient β and the absorption factor $I_j(t)$ is to ensure that the location of UGV (i.e. the current viewpoint, as shown in Fig. 1 has a smaller diffused pheromone than surrounding viewpoints. Let

$$\beta = \min(u_k(t) : k = 1, 2, \dots, N \wedge u_k(t) \neq 0) \text{ and}$$

$$I_j(t) = \begin{cases} 1, & \text{if } v_j \in V_c \\ 0, & \text{if } v_j \notin V_c \end{cases}, \quad (12)$$

where V_c is the viewpoint where the UGV is arriving.

Synthetic pheromone represents the pheromone finally possessed by v_j , which is a variable formed by the combination of releasing pheromone and diffused pheromone. The diffused pheromone from different viewpoints essentially reflects the monitoring uncertainty benefits that can be obtained after arriving at different viewpoints according to the current model state. In other words, the larger the synthetic pheromone, the greater the influence of the viewpoint on the global monitoring uncertainty. Therefore, the synthetic pheromone of the v_i is

$$p_i^s = \max(p_i^r, p_i^d). \quad (13)$$

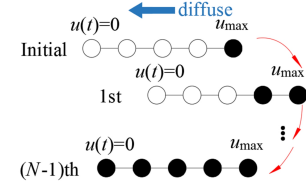


Fig. 2 The diffusion of pheromone on a chain. The solid viewpoint indicates that the iteration calculation of the synthetic pheromone at this viewpoint is completed, and the value will not be changed in the next iteration.

Algorithm 1: Pheromone Diffusion

Input: $u(t), V_c, t_{\lim}, v_u, O_v, W, D$, neighborhood set A_v
Output: synthetic pheromone p^s , diffusion source v_{ms}

- 1 **for** each viewpoint sign i **do**
- 2 $\|p_i^r\| \leftarrow$ calculate releasing pheromone through (8);
- 3 $p^s \leftarrow p^r, \beta \leftarrow \min(u(t) : u(t) \neq 0);$
- 4 **for** $k \in \mathbb{Z}$: from 1 to N **do**
- 5 **for** each viewpoint sign i **do**
- 6 $\|$ **if** $u_i(t) \neq u_{\max}$
- 7 $\|$ **for** $j \in \mathbb{Z}$: $v_j \in A_{vi}$ **do**
- 8 $\|$ $\|$ $\|$ $p_j^d \leftarrow$ calculate diffusion pheromone by (9);
- 9 $\|$ $\|$ $\|$ $p_j^s = \max(p_j^r, p_j^d);$

C. Synthetic Pheromone

Eq. (9) - (13) show that synthetic pheromone cannot be obtained by one calculation, because the diffusion of pheromone is bidirectional - the diffused pheromone at a certain viewpoint is also affected by its own releasing pheromone. We have developed a simple pheromone diffusion algorithm to iteratively calculate the synthetic pheromone of each viewpoint, as shown in **Algorithm 1**. After multiple iterations, the pheromone of the viewpoint adjacent to the major diffusion source will no longer change. The viewpoint where the UGV is located has the lowest

releasing pheromone, so the synthetic pheromone of all viewpoints will be finally passed to this viewpoint. In particular, considering the chain topology, as shown in Fig. 2, the viewpoints with the maximum and minimum uncertainties are arranged at both ends of the chain. At this time, the synthetic pheromone at the viewpoint where the UGV is located can be obtained at most $N-1$ time iterations.

IV. PHEROMONE-DIFFUSION-BASED CONSCIENTIOUS REACTIVE PERSISTENT SURVEILLANCE

A. Decision Rule

In the reactive architecture, the UGV only makes decisions based on the information from surrounding viewpoints. As mentioned earlier in this paper, the synthetic pheromone actually reflects the influence of the viewpoint on the global uncertainty. Taking into account the time consumption of the UGV moving along the edge, we set the pheromone payoff as the amount of decision-making about the forward direction:

$$A_j = p_j^s - \frac{c_L \|D_{i,j}\|}{v_u t_{\lim} \sigma_i}, \quad (14)$$

where A_j is the pheromone payoff of the UGV to the j -th viewpoint. The method of considering time or path cost in decision-making is also called "Conscientious" method [16]. The UGV will select the viewpoint with the greatest payoff among all adjacent viewpoints as the target, that is, the UGV will select the direction with the largest pheromone gradient as the moving direction $\theta(t)$

$$\theta(t) : v_c \rightarrow \arg \max A_j. \quad (15)$$

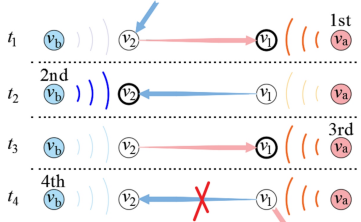


Fig. 3 The judgment of Multi-source Deadlock. Two consecutive trackbacks mean that there is a secondary diffusion source near the UGV, which should be eliminated to avoid local optimum. v_a and v_b are the diffusion sources before UGV reaches v_1 and v_2 , respectively. At the time t_1 , attracted by v_a (1st), UGV arrives at v_1 . At the time t_2 , UGV arrives at v_2 , under the attraction of v_b (2nd). Then at time t_3 , UGV returns to v_1 attracted by v_a (3rd). If there is no any intervention, UGV will turn back to v_2 again under the attraction of v_b .

Algorithm 2: Local Optimum Avoidance

Input: $u(t)$, d_c , d_L , O_v , S_d , coordinate set V
Output: O_v^0 , $u^0(t)$

- 1 $a \leftarrow S_d(1)$; $d_{op} \leftarrow$ the distance from v_a to UGV;
- 2 **if** $d_c < d_{op} < d_L$ **% Attractive force plummet**
- 3 $O_v^0 \leftarrow O_v^0$; $u^0(t) \leftarrow u(t)$; $u_a^0(t) \leftarrow 1$; $u^0(t) \leftarrow u^0(t)$;
- 4 **elseif** $a = S_d(3) \& a \neq S_d(2)$ **% Multi-source deadlock**
- 5 $b \leftarrow S_d(2)$;
- 6 **if** $u_a(t) \neq 0$
- 7 **for** $i \in \mathbb{Z} : v_i \in O_v^0$ **do**
- 8 $O_v^0 \leftarrow O_v^0$; $u^0(t) \leftarrow u(t)$; $u_a^0(t) \leftarrow 0$; $u^0(t) \leftarrow u^0(t)$;
- 9 **else**
- 10 $O_v^0 \leftarrow O_v^0$; $u^0(t) \leftarrow u(t)$;

B. Local Optimum Avoidance

Although the synthetic pheromone contains global information, the complex topology of the road network and the limited detection range of UGV may still cause the local optimum - UGV frequently backtracking between two viewpoints. Regarding each viewpoint that produces releasing pheromone as a source of attractive force in an artificial potential field, the reactive method will also face the following two risks of causing the local optimum. The first risk occurs when the UGV approaches the major diffusion source, i.e. $d_c < d_{ms} < d_L$, where d_{ms} is the distance from the major diffusion source to the UGV. At this time, the monitoring uncertainty of the last major diffusion source will greatly reduce. If the new major diffusion source attracts the UGV from the opposite direction, the UGV will fall into a local optimum. The second risk occurs when there are multiple sources of diffusion of similar intensity in the road network. At this time, although the last diffusion source remains unchanged, the secondary diffusion source closer to the UGV generates an attractive force equivalent to the strength of the last major diffusion source, causing the UGV to backtrack between the two viewpoints. These two risks are respectively called "Attractive Force Plummet" and "Multi-source Deadlock".

The solution for the first risk is as follows. Use the updated observable viewpoints set O^n and the updated uncertainty $u^n(t)$ for generating the synthetic pheromone when $d_c < d_{ms} < d_L$, where O^n is obtained under the condition of $d_L^n = 2d_c^n = e_{\min}$, e_{\min} is the minimum distance between any two viewpoints, and $u^n(t)$ is obtained by modifying the monitoring uncertainty of the major diffusion source $u_{ms}^n(t) = 1$.

Algorithm 3: PD-CRPS

Load: Undirected graph $G=(V, E, D, W)$, function f_c ;
Input: Task duration T , initial position X_0 , t_d , t_{\lim} , v_u ;
Output: Trajectory of UGV X_T ;

- 1 $O_v, O_v^n \leftarrow$ The observable viewpoints set;
- 2 $S_d \leftarrow$ a FIFO queue that holds three elements;
- 3 **for** each t in T at intervals of dt **do**
- 4 $| u(t) \leftarrow$ monitoring uncertainty of each point i ;
- 5 **if** the UGV arrive at one of viewpoints
- 6 **|| if** all viewpoints have been fully monitored
- 7 **|||** $O_v^0, u^0(t) \leftarrow$ Local Optimal Avoidance;
- 8 **|||** $p^s, v_{ms} \leftarrow$ Pheromone Diffusion [$O_v^0, u^0(t)$];
- 9 **|||** $S_d(1) \leftarrow v_{ms}$ in principle of first-in first-out;
- 10 **||| for** $j \in \mathbb{Z} : v_j \in A_{v_i}$ **do**
- 11 **||| |** $A_j(t) \leftarrow$ calculate the payoff through (14);
- 12 **||| |** $\theta(t) \leftarrow \arg \max(A_j(t))$;
- 13 **|||** Calculate $P(t+t_d)$ through (1);

The solution for the second risk is as follows. When the UGV continuously backtracks, if the major diffusion source remains unchanged, temporarily close the major diffusion source, i.e., use the updated uncertainty $u^n(t)$ to generate the synthetic pheromone, which is obtained by modifying the uncertainty of the major diffusion source $u_{ms}^n(t) = 0$.

Algorithm 2 shows the algorithm we developed to avoid the local optimum. The purpose of this algorithm is to provide **Algorithm 1** with the input of observable viewpoints set and monitoring uncertainty required for each calculation. As shown in Fig. 3, in order to judge whether to fall into the local

optimum, the algorithm needs the positions of the major diffusion source in the first three decisions, which is represented by the diffusion source matrix S_d .

C. Algorithm Implementation

Algorithm 3 shows the pseudo-code of PD-CRPS. The algorithm does not set special rules to suppress backtracking of the UGV but affects the decision-making by modifying environmental parameters. Since the algorithm adopts a reactive architecture, its computational time complexity is determined by the pheromone diffusion algorithm, which is $O(\max(\|A_i\|) \cdot N^2)$ and far less than $O(\max(\|O_i\|) \cdot N^4)$ of RPS, where $(\max(\|O_i\|) = i \in [1, N], i \in \mathbb{N})$.

V. Simulation Experiment

A. Simulation Cases

To intuitively compare the methods, the same simulation cases as in [4] are used. Four road network models with different topologies and obstacles are also used in the section.

The four road networks with different topologies or observation obstacles, as shown in Fig. 7, are marked respectively as $G1$, $G2$, $G3$, and $G4$ from left to right. In all road networks, the minimum Euclidean distance between two adjacent viewpoints is 3 m, while the maximum is 15 m.

The value of the observation radius is set as 10 m, 20 m, and 30 m, respectively. The corresponding cases are marked as $P1$, $P2$, and $P3$. The reason is to ensure that the UGV can detect at least two viewpoints at the same time.

The two monitoring weight matrices are set as follow. All elements of the first matrix $W1$ are 1, which means that the weights of the viewpoints are the same. In the second matrix $W2$, eight of all viewpoints are randomly selected and assigned values between 1 and 2.

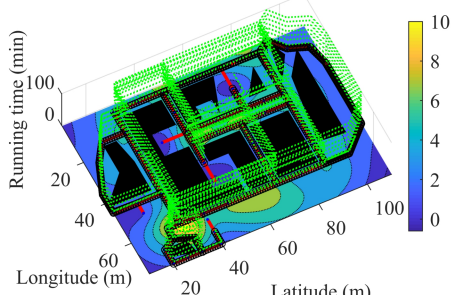


Fig. 4 The surveillance level of the road network with observation obstacles. The blue dots represent the viewpoints, and the red line segments are edges. The black polygons are observation obstacles, UGV cannot see through them. Different fill colors indicate different surveillance levels. The lighter the color, the longer the area is fully monitored. The green dots represent the trajectory of the UGV, and the black circles are the footprints of the UGV. The results are obtained under the condition of $P1$, $W2$, and $G1$.

A. Simulation Results and Performance Analysis

The performance of the algorithm was tested based on different simulation conditions, and the algorithm was evaluated in terms of effectiveness and accuracy. All the following results are from a desktop computer with Intel Core i7-7700 (3.6GHz) and Samsung DDR4 (4GB) memory. The basic simulation conditions are as follows: $d_L = 2d$, $dt = 1$ s, $T = 100$ min, $v_u = 1$ m/s, $t_{lim} = 1000$ s, $p_m = 0$, and $c_L = 0.25$. In order to reduce the influence of algorithm randomness, all results of the criteria are obtained through 10 calculations.

1) *Effectiveness*: Fig. 4 qualitatively shows that the

algorithm can solve the RPSP in the environment with observation obstacles. Whether there is an observation obstacle between UGV and viewpoint can be determined by whether the virtual line between them intersects any boundary of all polygon obstacles. It can be qualitatively seen that the UGV has not arrived at all viewpoints while the detection time of all viewpoints is greater than 0, and some weighted viewpoints have more time to be detected. This shows that the UGV has achieved persistent surveillance of all viewpoints without traversing all viewpoints. This ability is not possessed by the patrolling method.

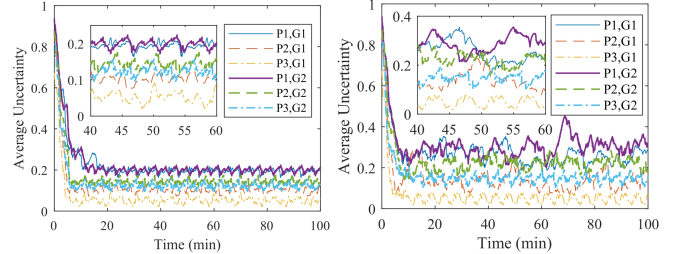


Fig. 5 The law of monitoring uncertainty over time under different conditions. a) and b) are obtained under conditions of $W1$ and $W2$ respectively.

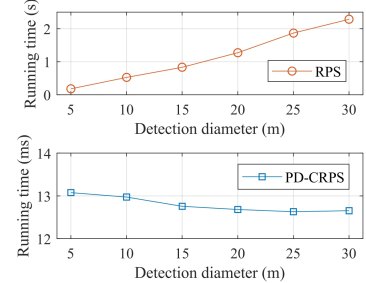


Fig. 6 The running time of different algorithms when making a decision. The time The results are obtained under the condition of $G1$ and $W1$.

Fig. 5 - 6 quantitatively shows the ability of the algorithm to efficiently solve the RPSP. As shown in Fig. 5, the average uncertainty shows a rapid decline and then stabilizes with small fluctuations, which indicates that the algorithm drives the UGV to reach a stable surveillance state after a rapid exploration, and even a stable cycle state. For example, under the conditions of $P2$, $G1$ and $W1$, the average uncertainty drops rapidly to 0.0857 at 344 s and oscillates periodically from 0.0724 to 0.1247 until the end of the mission. As the detection ability increases from 10 m to 30 m, the average uncertainty gradually decreases from 0.1996, 0.1038, to 0.0517 under the conditions of $G1$ & $W1$ and from 0.2528, 0.1320, to 0.0483 under the conditions of $G1$ & $W2$.

Fig. 6 tests the time it takes for the algorithm to make a decision and compares it with the running time of RPS. The running time of the algorithm in this paper is much shorter than that of RPS, and it has little to do with the detection ability of UGV. Especially, when the observation radius is equal to 30 m, the running time of one decision-making using RPS is more than 2 s, while PD-CRPS takes only 0.0127 s.

2) *Accuracy*: The comparison with four existing feasible methods shows the accuracy of the proposed algorithm in solving RPSP. The first two methods are designed based on the classical reactive patrolling methods called Conscientious Reaction (CR) and Heuristic Conscientious Reaction (HCR) [28]. The third comparison method is GLInG [23], a patrolling algorithm based on pheromone diffusion. Here,

these methods are modified to adapt to RPSP. Specifically, the amount of decision-making of CR and GLInG are set as the sum of the uncertainty of all observable viewpoints, and

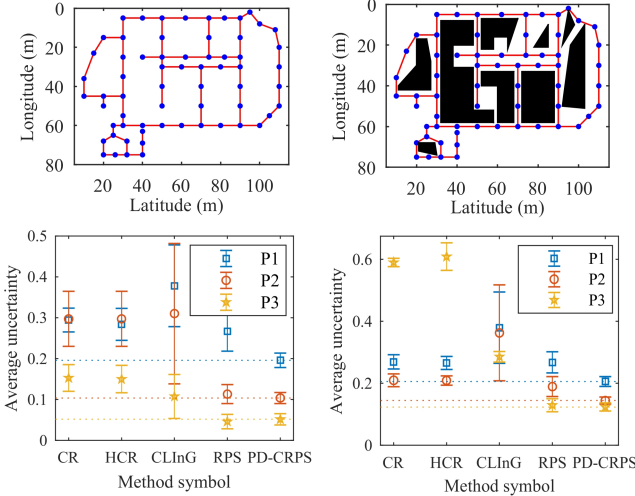


Fig . 7 The accuracy of the different algorithms in four different road networks. The four performance comparison charts below correspond to the four road networks above. The dashed line parallel to the abscissa represents the result of PD-CRPS for different detection abilities.

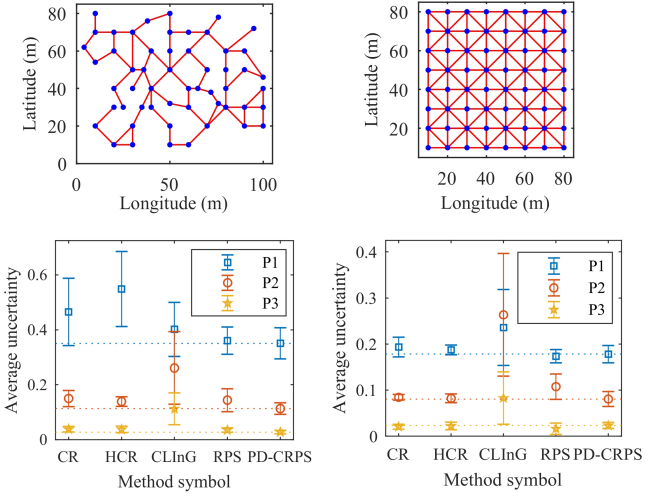
As shown in Fig. 7, the results of the five methods in the road network models with different topology, viewpoint distribution, and observation obstacles show the advantages of this proposed method in terms of accuracy. The PD-CRPS has achieved the best results than other methods in the irregular road networks (as shown in Fig. 7 a) – c), even ahead of RPS when the static coverage is more smaller than the area of the road network, e.g., PD-CRPS improves approximately the calculation accuracy by 24% under conditions of $G1$, $P1$ and $W1$. In the regular road network (as shown in Fig. 7 d), the PD-CRPS does not have obvious advantages in calculation accuracy. This indicates that the PD-CRPS can replace RPS in the scene of UGV monitoring an irregular road network with a small coverage area.

Compared with Fig. 7 e) and f), PD-CRPS still maintains the accuracy advantage compared with other methods after adding observation obstacles. In addition, PD-CRPS is more stable than conventional reactive methods without global estimation ability in complex environment. This conclusion can be seen from the following special phenomena. After increasing the observation obstacle, the reactive method without global estimation can achieve better monitoring effect under some conditions. This is because the observation obstacles reduce the number of observable viewpoints. Several viewpoints that would make UGV fall into local optimum just no longer block UGV. But with the increase of d_c , UGV gets stuck in a more serious local optimum. It can be seen that the reactive method based on local information alone cannot guarantee stable performance.

VI. DISCUSSION AND CONCLUSION

The detection ability of the UGV in this paper is modeled as a layered model - the position within the field of view that is close to the UGV can be fully monitored, the distant location is partially monitored, and the rest cannot be monitored. However, PD-CRPS is not limited to this detection model. In the diffusion of pheromone, the method in this paper considers the observable viewpoints, that is, only

that of HCR takes the path cost into consideration on the basis of the modified CR. The fourth comparison method is the cognitive persistent surveillance algorithm RPS [4].



considers the influence of the UGV on the position that can be fully monitored. But when calculating the monitoring uncertainty, the influence of the UGV on all positions is monitored. Therefore, for any sensor detection model, as long as the model has the assumption that “the UGV can fully detect events occurring at a sufficiently close location”, the method in this paper is applicable. However, this feature is not only the advantage of the method in this paper in terms of application range, but also the disadvantage of calculation accuracy. Because the detection effect of distant locations is not considered when pheromone diffusion and decision-making, the calculation accuracy may be affected.

Although the persistent surveillance problem of time-invariant systems is considered in this paper, the proposed method can work in dynamic environment. Based on the surveillance effect of current environment, sensor ability, and road network topology, PD-CRPS selects the neighbor which has the greatest impact on the global surveillance effect as the path point at the next moment. Therefore, no matter whether the sensor detection ability and observation obstacles are fixed or not, this method can find the best choice based on the current state.

The decision-making amount of the PD-CRPS is based on the relative value of monitoring uncertainty (divided by the number of the observable viewpoints when calculating the releasing pheromone) rather than the real uncertainty of a certain viewpoint. Therefore, the PD-CRPS is particularly suitable for road network with irregular topological structures and uneven distribution of viewpoints similar to real road network models, and for the scene where the static coverage of the UGV is much smaller than the coverage area of the road network. Because in these scenes, the difference in relative monitoring uncertainty information between different viewpoints is greater than that in a regular road network.

In future work, we will consider more detection models of sensor and dynamic environments. At the same time, we will consider extending the method in this paper to the persistent surveillance of the road network by the UGV group.

REFERENCES

- [1] L. Freda, M. Gianni, F. Pirri, A. Gawel, R. Dube, R. Siegwart, and C. Cadena. "3D multi-robot patrolling with a two-level coordination strategy", *Autono. Robots*, vol. 43, no. 7, pp. 1747-1779, 2019.
- [2] S. C. Mohamed, S. Rajaratnam, S. T. Hong and G. Nejat. "Person finding: an autonomous robot search method for finding multiple dynamic users in human-centered environments", *IEEE Trans. Autom. Sci. Eng.*, vol. 17, no. 1, pp. 433-449, Jan 2020.
- [3] K. E. C. Booth, C. Piacentini, S. Bernardini, and J. C. Beck. "Target search on road networks with range-constrained UAVs and ground-based mobile recharging vehicles", *IEEE Robot. Autom. Letters*, vol. 5, no. 4, pp. 6702-6709, Oct 2020.
- [4] T. Wang, P. F. Huang, G. Q. Dong, "Modeling and path planning for persistent surveillance by unmanned ground vehicle", *IEEE Trans. Autom. Sci. Eng.*, doi: 10.1109/TASE.2020.3013288, 2020.
- [5] T. Sakamoto, S. Bonardi, and T. Kubota. "A Routing Framework for Heterogeneous Multi-Robot Teams in Exploration Tasks", *IEEE Robot. Autom. Letters*, DOI 10.1109/LRA.2020.3016285, 2020.
- [6] M. Hassan and D. Liu. "PPCPP: a predator-prey-based approach to adaptive coverage path planning", *IEEE Trans. Robot.*, vol. 36, no. 1, pp. 284-301, 2020.
- [7] Y. Wang, Y. Wei, X. Liu, N. Zhou, and C. G. Cassandras, "Optimal Persistent Monitoring Using Second-Order Agents With Physical Constraints," *IEEE Trans. Autom. Control*, vol. 64, no. 8, pp. 3239-3252, 2019.
- [8] O. Thakoor, J. Garg, and R. Nagi. "Multiagent UAV Routing: A Game Theory Analysis With Tight Price of Anarchy Bounds", *IEEE Trans. Autom. Sci. Eng.*, vol. 17, no. 1, pp.100-116, 2020.
- [9] D. Panagou, D. M. Stipanovic, and P. G. Voulgaris. "Distributed dynamic coverage and avoidance control under anisotropic sensing", *IEEE Trans. Control Net. Syst.*, vol. 4, no. 4, pp. 850-862, 2017.
- [10] T. Alam, M. M. Rahman, P. Carrillo, L. Bobadilla, and B. Rapp. "Stochastic multi-robot patrolling with limited visibility", *J. Intell. Robot. Syst.*, vol. 97, no. 2, pp. 411-429, 2020.
- [11] X. Tan and B. Jiang. "An improved algorithm for computing a shortest watchman route for lines", *Inform. Proces. Letters*, vol. 131, pp. 51-54, 2018.
- [12] L. Huang, M. C. Zhou, K. R. Hao, and E. Hou. "A survey of multi-robot regular and adversarial patrolling", *IEEE/CAA J. Autom. Sinica*, vol. 6, no. 4, pp. 894-903, 2019.
- [13] N Nigam. "The Multiple Unmanned Air Vehicle Persistent Surveillance Problem: A Review", *Machines*, vol. 2, no. 1, pp. 13-69, 2014.
- [14] A. Otto, N. Agatz, J. F. Campbell, B. L. Golden, and E. Pesch. "Optimization approaches for civil applications of unmanned aerial vehicles (UAVs) or aerial drones: A survey", *Networks*, vol. 72, no. 4, pp. 411-458, 2018.
- [15] D. Portugal and R. Rocha, "A survey on multi-robot patrolling algorithms," in *Doctoral Conf. Comput., Elect. Indust. Syst.*, Springer, 2011, pp. 139-146.
- [16] D. Portugal and R. P. Rocha, "Multi-robot patrolling algorithms: examining performance and scalability," *Adv. Robotics*, vol. 27, no. 5, pp. 325-336, Apr 2013.
- [17] S. J. Chung, A. A. Paranjape, P. Dames, S. J. Shen, and V. Kumar. "A survey on aerial swarm robotics", *IEEE Trans. Robot.*, vol. 34, no. 4, pp. 837-855, 2018.
- [18] A. Wallar, E. Plaku, and D. A. Sofge. "Reactive Motion Planning for Unmanned Aerial Surveillance of Risk-Sensitive Areas," *IEEE Trans. Autom. Sci. Eng.*, vol. 12, no. 3, pp. 969-980, Jul 2015.
- [19] O. Arslan and D. E. Koditschek, "Sensor-based reactive navigation in unknown convex sphere worlds," *Int. J. Robot. Res.*, vol. 38, no. 2-3, pp. 196-223, Mar 2019.
- [20] M. P. Jose, M. Eduardo, S. Carlos, L. Sergio, "Distributed coverage estimation and control for multirobot persistent tasks," *IEEE Trans. Robot.*, vol. 32, no. 6, pp. 1444-1460, Dec 2016.
- [21] P. A. Sampaio, R. D. Sousa, and A. N. Rocha, "Reducing the range of perception in multi-agent patrolling strategies," *J. Intell. Robot. Syst.*, vol. 91, no. 2, pp. 219-231, Aug 2018.
- [22] I. A. Wagner, Y. Altshuler, V. Yanovski, and A. M. Bruckstein, "Cooperative cleaners: A study in ant robotics," *Int. J. Robot. Res.*, vol. 27, no. 1, pp. 127-151, Jan 2008.
- [23] H. N. Chu, A. Glad, O. Simonin, F. Sempe, and F. Charpillet. "Swarm Approaches for the Patrolling Problem, Information Propagation vs. Pheromone Evaporation", in 19th *IEEE Int. Conf. Tools Artif. Intell. (ICTAI)*, 2007.
- [24] W. N. Chen, D. Z. Tan, Q. Yang, T. L. Gu, and J. Zhang. "Ant colony optimization for the control of pollutant spreading on social networks", *IEEE Trans. Cybern.*, vol. 50, no. 9, pp. 4053-4065, 2020.
- [25] G. J. Han, Z. R. Zhou, T. W. Zhang, H. Wang, and M. Guizani. "Ant-colony-based complete-coverage path-planning algorithm for underwater gliders in ocean areas with thermoclines", *IEEE Trans. Vehi. Tech.*, vol. 69, no. 8, pp. 8959-8971, 2020.
- [26] J. J. Yu, S. Karaman, and D. Rus, "Persistent Monitoring of Events With Stochastic Arrivals at Multiple Stations," *IEEE Trans. Robot.*, vol. 31, no. 3, pp. 521-535, Jun 2015.
- [27] X. C. Lin and C. G. Cassandras, "An Optimal Control Approach to the Multi-Agent Persistent Monitoring Problem in Two-Dimensional Spaces," *IEEE Trans. Autom. Control*, vol. 60, no. 6, pp. 1659-1664, Jun 2015.
- [28] A. Machado, G. Ramalho, J.-D. Zucker, and A. Drogoul, "Multi-agent Patrolling: An Empirical Analysis of Alternative Architectures," in *Multi-Agent-Based Simulation II*, New York, USA, 2003, pp. 155-170.